Comparison of large-scale field-aligned currents under sunlit and dark ionospheric conditions

S. Ohtani

Johns Hopkins University Applied Physics Laboratory, Laurel, Maryland, USA

G. Ueno and T. Higuchi

Institute of Statistical Mathematics, Tokyo, Japan

[1]   The present study statistically compares large-scale field-aligned currents (FACs) under sunlit and dark ionospheric conditions. A total of $\sim$74,000 auroral oval crossings are selected from magnetic field measurements from the DMSP F7 and F12 to F15 satellites. For the dayside FAC it is reconfirmed that both current intensity and density are statistically larger in the illuminated events than in the unilluminated events. As for the nightside FAC, in contrast, a few important features become clear for the first time, which can be summarized as follows: (1) At $20 \leq \mathrm{MLT} < 02$ both R1 and R2 intensities tend to be larger when the ionosphere is dark than when it is sunlit. (2) Although dependence on the ionospheric condition is less clear for the FAC density, a systematic preference of the occurrence of strong FACs for the dark ionosphere can be found for both R1 and R2 currents in the dusk-to-premidnight ($16 \leq \mathrm{MLT} < 22$) sector and for the R1 current in the postmidnight sector ($00 \leq \mathrm{MLT} < 02$). (3) For both FAC intensity and density the difference between the illuminated and unilluminated events tends to increase with increasing geomagnetic activity as measured by the IMF B_Z component. Result 1 can be partially explained in terms of the interhemispheric asymmetry of the magnetospheric configuration, which, however, should not affect the FAC density. Therefore result 2 strongly suggests that the solar-induced conductivity controls the M-I coupling in a different way in certain nightside MLT sectors than in dayside sectors.

Citation: Ohtani, S., G. Ueno, and T. Higuchi (2005), Comparison of large-scale field-aligned currents under sunlit and dark ionospheric conditions, *J. Geophys. Res.*, *110*, A09230, doi:10.1029/2005JA011057.

1.   Introduction

[2]   The ionospheric conductivity controls the electromagnetic coupling between the magnetosphere and ionosphere. On the dayside the average intensity of field-aligned currents (FACs) is larger in summer than in winter by a factor of $2-3$ [*Fujii et al.*, 1981; *Fujii and Iijima*, 1987; *Christiansen et al.*, 2002; *Haraguchi et al.*, 2004; *Ohtani et al.*, 2005]. Polar distributions of the FAC density [*Weimer*, 2001; *Papitashvili et al.*, 2002] also indicate stronger dayside FACs in the summer hemisphere than in the winter hemisphere. This annual variation (or interhemispheric difference) can be attributed to the solar EUV contribution to the ionospheric conductivity, which is a main cause of ionospheric ionization. The dayside ionospheric conductivity is higher when the ionosphere is sunlit than when it is dark. Thus it should be reasonable that more electric current flows through the sunlit ionosphere than through the dark ionosphere. On the dayside, intense electron acceleration events are also observed more often under the sunlit condition [*Newell et al.*, 1996]. Thus it seems that higher background conductivity results in closer electromagnetic coupling between the magnetosphere and the ionosphere.

[3]   However, in the dusk-to-midnight sector, where auroral acceleration is most common [e.g., *Lin and Hoffman*, 1979], the occurrence of intense electron precipitation clearly prefers the dark ionosphere to the sunlit ionosphere [*Newell et al.*, 1996]. It is also known that nightside aurora tends to be brighter [*Liou et al.*, 1997; *Shue et al.*, 2001] and the acceleration energy is higher [*Liou et al.*, 2001] when the foot point is dark than when it is sunlit. Preferences for the unilluminated ionosphere can also be found for the occurrence of upward electron beams [*Elphic et al.*, 2000; *Cattell et al.*, 2004], strong electric field [*Bennett et al.*, 1983; *Marklund et al.*, 1997], and accelerated ion precipitation [*Newell et al.*, 2005].

[4]   It is widely considered that for the upward FAC, the FAC density is positively correlated with the field-aligned potential drop [*Knight*, 1973], which has been affirmatively tested on the basis of satellite observations [*Lyons*, 1980, 1981; *Olsson et al.*, 1998]. Since the occurrence of intense auroral acceleration events prefers the dark ionosphere, it is expected that the density of the upward FAC is higher under the dark condition than under the sunlit condition. On the other hand, it seems to be counterintuitive that more current

flows through the dark ionosphere than through the sunlit ionosphere because the solar-induced ionospheric conductivity should be lower for the former than for the latter.

[5] A few studies examined nightside large-scale FACs in terms of either season or solar illumination [*Fujii et al.*, 1981; *Fujii and Iijima*, 1987; *Christiansen et al.*, 2002]. However, the results are not conclusive presumably because of limited spatial or temporal coverage of data sets. Recently *Ohtani et al.* [2005, hereinafter referred to as paper 1] examined the intensities of region 2 (R2) and region 1 (R1) currents [*Iijima and Potemra*, 1976] in terms of the dipole tilt angle. Whereas they found that the nightside R2 intensity tends to be larger in winter than in summer, they could not find any significant correlation for the R1 intensity.

[6] In the present study we systematically compare the intensity and density of large-scale FACs under sunlit and dark ionospheric conditions. We previously applied a procedure developed by *Higuchi and Ohtani* [2000a, 2000b] to nearly 19 years' worth of DMSP magnetic field data [*Rich et al.*, 1985] and identified FAC structures for about 185,000 auroral oval crossings. We use the same data set for the present study. In section 2 we describe the data set and event selection, and in section 3 we examine the FAC intensity and density for different ionospheric conditions for different MLT sectors. Results are discussed in section 4. Section 5 is a summary.

2. Data Set and Event Selection

[7] In the present study we use 1-s magnetometer data obtained from triaxial fluxgate magnetometers [*Rich et al.*, 1985] onboard the DMSP F7 (period of data used for this study: December 1983 to January 1988), F12 (September 1994 to November 2000), F13 (March 1995 to July 2000), F14 (December 1997 to September 2000), and F15 (December 1999 to September 2000) satellites. This is the same data set as used in paper 1. All DMSP satellites have Sun-synchronous orbits (F13 approximately in a dawn-dusk orientation and others in prenoon-premidnight orientations) at about 840 km in altitude with orbital periods of approximately 100 min. See Figure 1 of paper 1 for the combined orbital coverage of those satellites in different hemispheres.

[8] *Higuchi and Ohtani* [2000a, 2000b] developed an automatic procedure to identify a structure of large-scale FACs along a satellite orbit, and we applied it to the DMSP data set. This procedure virtually fits line segments to a plot of the maximum variance component of horizontal magnetic field measurements. FAC structures were identified for about 185,000 auroral oval crossings. The MLT distribution of the occurrence of FAC crossings is shown in Figure 2 of paper 1.

[9] We selected "illuminated (-foot point)" and "unilluminated (-foot point)" events on the basis of the solar zenith angle, χ, at the magnetic foot point at 110 km in altitude. If χ is less (larger) than $90°$ throughout an orbital segment during the entire crossing of FACs, that is, from the equatorwardmost point of the equatorwardmost FAC sheet to the polewardmost point of the polewardmost FAC, the crossing of each FAC sheet is selected as an illuminated (unilluminated) event. We emphasize that events were selected not on the basis of the ionospheric condition for each data point or each FAC sheet but on the basis of the ionospheric condition of the entire crossing of FACs along

an orbit irrespective of the number of FAC sheets. This strict condition for the event selection should be ideal for the present study because large-scale FACs are controlled by global as well as local electrodynamics.

[10] In addition, we required that the following conditions be satisfied for the automatic fitting: (1) α, the square root of the maximum to minimum ratio of two eigenvalues of the maximum variance analysis of two horizontal components, is larger than 2; (2) Φ_Z, the angle between the maximum variance orientation and the satellite cross-track direction, is less than $30°$; (3) R_{fit}, the ratio of the standard deviation of the residuals of the fitting to the magnitude of the magnetic change corresponding to the most intense FAC, is less than 10%. For the details of those parameters, see *Higuchi and Ohtani* [2000b].

[11] We selected a total of ∼74,000 events (counting a crossing of multiple FAC sheets as one event), and for each 2-hour MLT bin, we have at least a few hundred events and very often a few thousand events or even more. This unprecedented number of events is crucial for the present study. It is well known that large-scale FAC systems strongly depends on solar wind parameters (or geomagnetic activity), and the FAC intensity and density substantially vary from event to event, especially on the night side, depending on geomagnetic activity [e.g., *Iijima and Potemra*, 1976]. Let us consider the IMF B_Z component as a measure of geomagnetic activity. Its standard deviation is inferred to be 2 nT at most [e.g., *Borovsky and Funsten*, 2003]. On the night side, as will be shown later, we have more than 400 events irrespective of the ionospheric condition and the MLT sector. Hence the average of IMF B_Z for an individual subset is expected to be at maximum 0.1 nT $(= 2 \text{ nT}/(400)^{1/2})$, and it should be even smaller in most sectors. Therefore we can safely assume that the result of the following comparison between illuminated and unilluminated events is not affected by any significant bias of geomagnetic activity.

3. Ionospheric Condition at the Foot Point
3.1. FAC Intensity and Density

[12] In this section we examine how the FAC intensity and density depend on the ionospheric condition, i.e., whether or not the magnetic foot point is sunlit or dark. Following the convention, we refer to the equatorwardmost and second equatorwardmost FACs as R2 and R1 currents, respectively, and in the following, we focus on FACs with the flowing polarities consistent with the conventional MLT distribution [*Iijima and Potemra*, 1976]; such events compose an overwhelming majority (Figure 2 of paper 1). The sign of the FAC intensity/density is defined as positive (negative) if the current flows upward (downward). Thus the R1 current intensity/density is negative on the morning side and is positive on the evening side. The sign of the R2 current is the opposite to that of the R1 current at a given local time. Caution needs to be exercised for FACs in the midday sector, where the R2 current is often absent [*Iijima and Potemra*, 1978]; we will return to this issue later is this subsection.

[13] Figure 1 compares the occurrence ratio of the R1 current intensity for illuminated (solid) and unilluminated (shaded) events for each 2-hour bin of MLT. Here the MLT
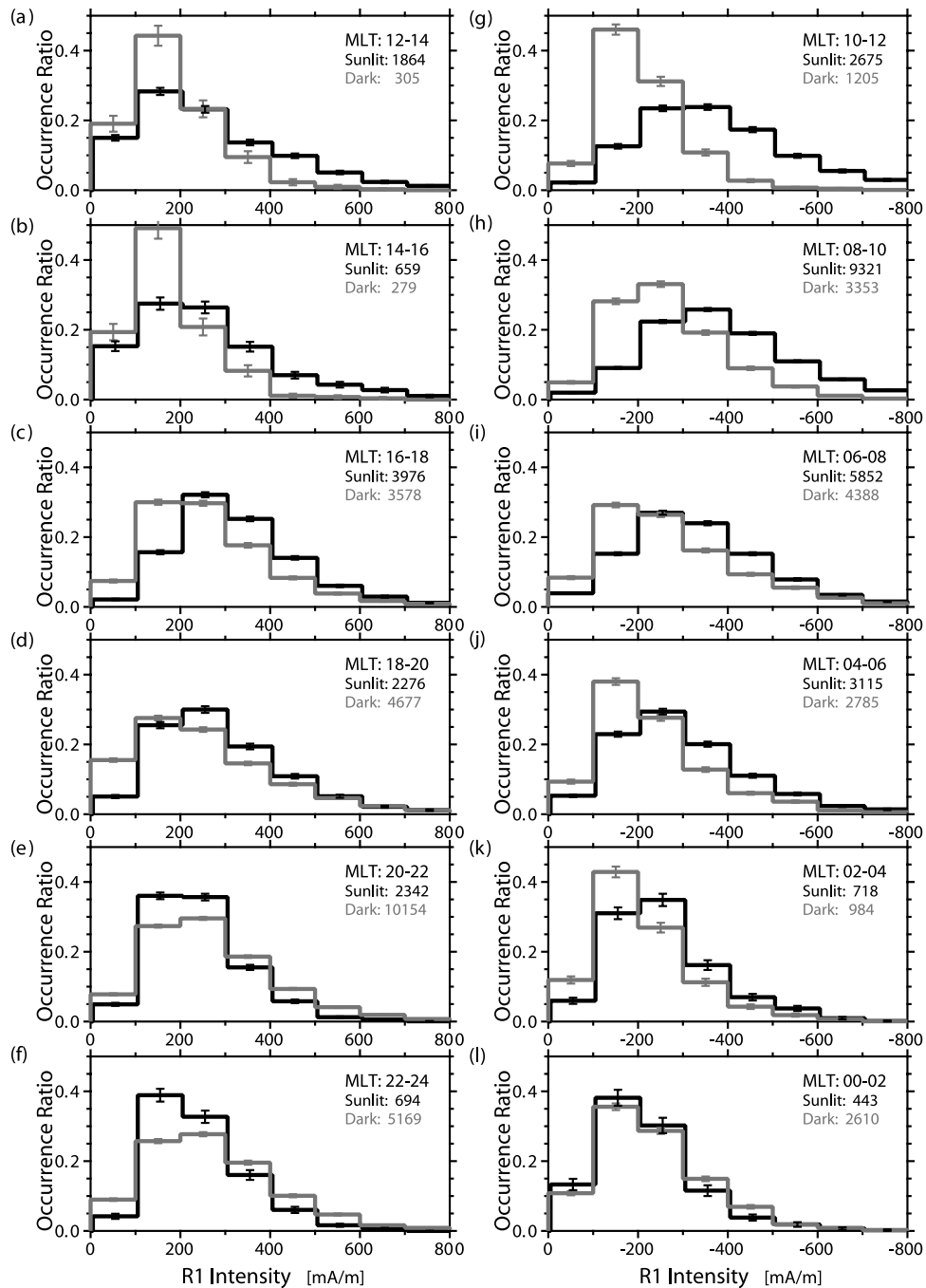
Figure 1. Occurrence ratio of the R1 current intensity for each 2-hour bin of MLT on (a–f) the evening (MLT: 12–24) and (g–l) morning (MLT: 00–12) sides. The solid and shaded lines are for the illuminated and unilluminated events, respectively. The numbers of events are inserted at the top right corner of each panel. For the downward FACs the horizontal axis is inverted.

of each event is defined as the mean of MLT's at the start and end points of the FAC crossing. Magnetic coordinates used in this study are in the Altitude Adjusted Corrected Geomagnetic (AACGM) Coordinate system, which was previously known as the PACE system [*Baker and Wing*, 1989]. Figures 1a–1f are for evening-side R1 currents, and the MLT increases downward from dayside ($12 \leq$ MLT < 14) to nightside ($22 \leq$ MLT < 24). Figures 1g–1l are for morning-side FACs, and the MLT increases upward from nightside ($00 \leq$ MLT < 02) to dayside ($10 \leq$ MLT < 12).

The FAC intensities used here are the values at the DMSP altitude. If the FAC has a sheet structure extending in the azimuthal direction, the FAC intensity is proportional to $r^{-1.5}$ (r: geocentric distance) for the dipole magnetic configuration; for example, the FAC intensity is expected to be 17% larger at 110 km in altitude than at the DMSP altitude. The horizontal scale is inverted for morning-side R1 currents, which flow downward. The numbers of events are inserted at the top right corner of each panel. Error bars indicate the range corresponding to $[p \cdot (1 - p)/N]^{1/2}$, the

expected error for the binominal distribution, where p is the occurrence ratio and N is the total number of events for each ionospheric condition in each MLT sector. Because of the large number of events available for the present study, some error bars are smaller than the thickness of the lines.

[14] On the dayside (Figures 1a, 1b, 1g, and 1h) the histogram is significantly different between the illuminated (solid) and unilluminated (shaded) events. For the unilluminated events, the distributions of the R1 intensity are confined in small ranges, whereas for the illuminated events, the R1 intensity is more widely distributed with larger average values. There is a recognizable difference in the distribution between prenoon and postnoon sectors, especially for the illuminated events. The distribution is more skewed toward small intensities in the postnoon sector. This apparent difference may be attributed to the characteristics of the DMSP orbits. In the postnoon sector, the DMSP spacecraft tend to skim the auroral oval (Figure 1 of paper 1). It is possible that the spacecraft cross FAC sheets preferably when the latitude of the auroral oval is high and therefore when the corresponding FAC is weaker.

[15] The difference between illuminated and unilluminated events is smaller at the flanks (Figures 1c, 1d, 1I, and 1j). Most interestingly, the tendency is just the opposite for the three sectors on the night side at $20 \leq$ MLT < 02 (Figures 1e, 1f, and 1l). In other words, the R1 current tends to be more intense when the ionospheric foot point is dark than when it is sunlit. Note that for those sectors, the difference between the illuminated and unilluminated events is systematic, and that intense (>400 mA/m) R1 currents are observed far more frequently under the dark condition than under the sunlit condition.

[16] Figure 2 shows the occurrence ratio of the R2 current intensity in the same format as Figure 1, which shows tendencies similar to what we found for the R1 current. On the dayside, the R2 current tends to be more intense when the ionospheric foot point is sunlit than when it is dark. The difference is less clear away from the midday sector, especially on the evening side. On the night side, intense FACs tend to take place more often when the ionosphere is dark. This opposite tendency can be found exclusively for $20 \leq$ MLT < 02 (Figures 2e, 2f, and 2l), the same MLT sector as we found a similar tendency for the R1 current, and it is more manifest for the R2 current than for the R1 current.

[17] We examined the ratio of the occurrence ratio for the unilluminated events to that for the illuminated events. Figures 3a and 3c superpose the results for all 2-hour-wide MLT sectors for the R1 and R2 current intensities, respectively. The vertical axis is given in the log scale. Absolute values are used for the intensities of downward FACs, and the range of the horizontal axis is limited because of large statistical uncertainty for large FAC intensities. The ratios for the aforementioned three MLT sectors are plotted by the solid lines with different marks, whereas the ratios for the other sectors are plotted by the shaded dash lines without distinction.

[18] For those three sectors the ratio tends to increase with the current intensity for both R1 and R2 currents; in other words, the preference for the dark ionosphere increases as the FAC intensity increases. For example, R1 currents with intensities larger than 400 mA/m are observed

a few times more frequently when the ionosphere is dark than when it is sunlit. The tendency is more or less the opposite in other sectors. This is consistent with the visual inspection of the histograms in Figures 1 and 2.

[19] Let us examine the occurrence of the FAC density. The FAC density is proportional to the slope of the magnetic variation during the crossing of a FAC sheet, and it can be calculated by dividing the FAC intensity by the width of the FAC sheet. We note in advance that determination of the width of FAC sheets, that is, determination of boundaries of FAC sheets, is subject to uncertainty caused by small-scale variations (see *Higuchi and Ohtani* [2000b, Figure 4] for examples of the segment fit), and therefore more caution is required for examining the FAC density; we will discuss more about the width of the FAC sheet in section 4.1. On the other hand, the FAC density, rather than the FAC intensity, is directly related to auroral acceleration [*Knight*, 1973], and it is more relevant to the local M-I coupling.

[20] Figures 4 and 5 show the occurrence ratio for the R1 and R2 current densities, respectively, in the same format as Figures 1 and 2. Here the current density is calculated for the DMSP altitude. The FAC density is proportional to the total magnetic field, which for the dipole field is inversely proportional to the cube of the radial distance; strictly speaking, it also depends on the magnetic latitude, which, however, does not change significantly along the field line below the DMSP altitude at high latitudes. The FAC density at an altitude of 110 km is inferred to be about 40% larger than at the DMSP altitude.

[21] The difference in the FAC density between the illuminated (solid) and unilluminated (shaded) events shows a tendency that is qualitatively similar to what we found for the FAC intensity, although it is less obvious (we will discuss this in section 4.1 in terms of the magnetospheric configuration). On the dayside, the FAC density is higher when the foot point is sunlit than when it is dark. The tendency is generally the opposite in the dusk-to-postmidnight sector. At $22 \leq$ MLT < 24 no systematic difference between the illuminated and unilluminated events can be recognized for the R1 (Figure 4f) or R2 (Figure 5f) density. At $00 \leq$ MLT < 02, the R1 density tends to be higher when the foot point is dark (Figure 4l), whereas the R2 density reveals the opposite tendency (Figure 5l).

[22] These nightside features can be confirmed in a different way in Figures 3b and 3d, which plot the ratio of the occurrence ratio under the dark condition to that under the sunlit condition for the R1 and R2 current densities, respectively. At $16 \leq$ MLT < 22 strong upward R1 currents tend to be observed more frequently when the ionospheric foot point is dark than when it is sunlit, and a similar preference can be found for strong downward R1 currents at $00 \leq$ MLT < 02. For R2 currents, the preference for the dark ionosphere can be found only for $16 \leq$ MLT < 22. Although there are a few exceptions, the preference is consistent in those sectors, which cannot be found for other sectors. Note also that the ratio is more confined for the FAC density than for the FAC intensity; the range of the vertical axis is different between the Figures 3a and 3c (FAC intensity) and Figures 3b and 3d.

[23] Interestingly, the evening-side demarcation between the dayside and nightside tendencies is located at an earlier MLT for the FAC density than for the FAC intensity. At
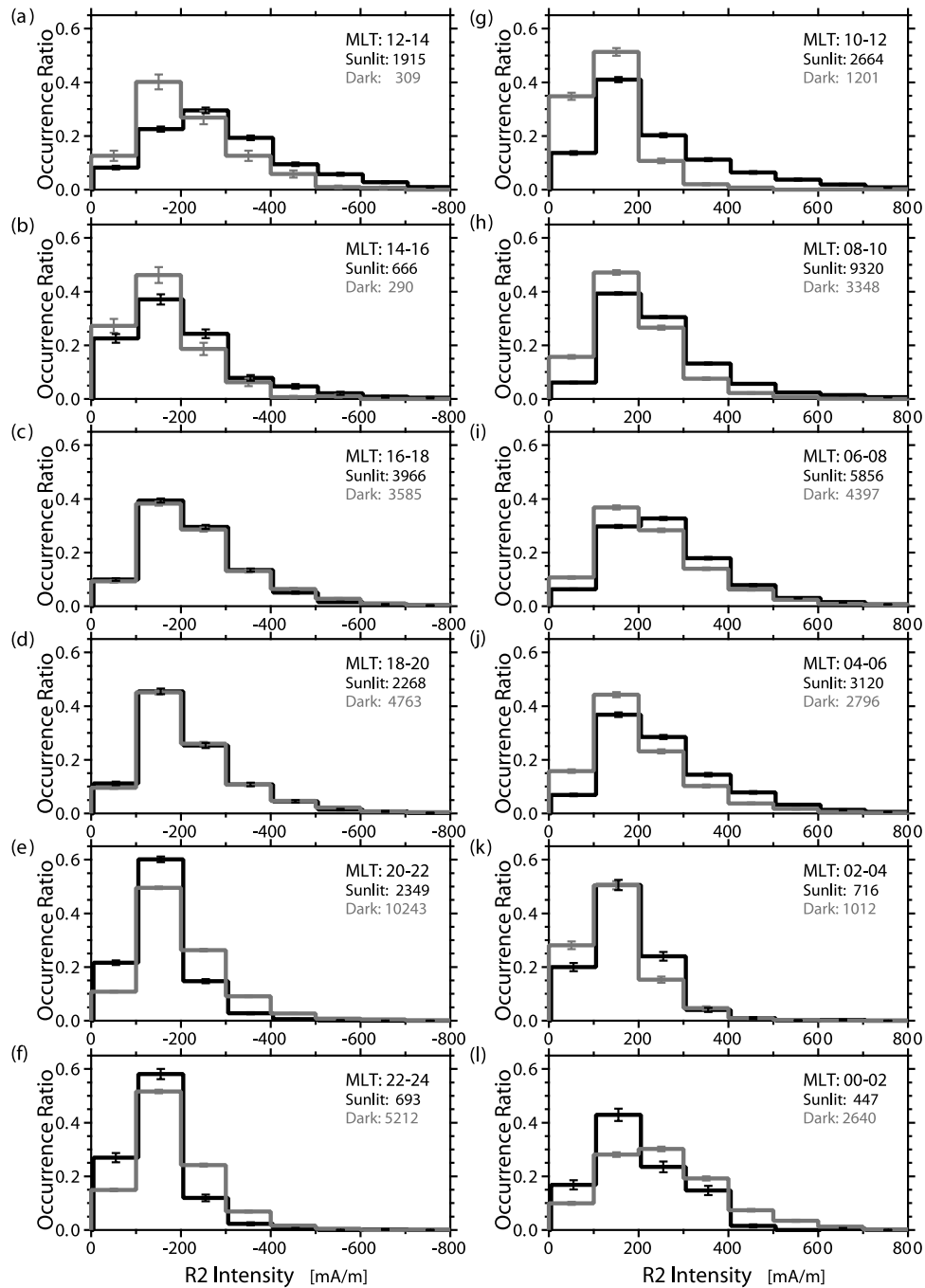
Figure 2. (a–l) Comparison of the R2 current intensity between the illuminated (solid) and unilluminated (shaded) events in the same format as Figure 1.

$18 \leq$ MLT < 20, both R1 and R2 densities tend to be higher when the ionospheric foot point is dark (Figures 4d and 5d), and a similar but less clear tendency can also be found at $16 \leq$ MLT < 18 (Figures 4c and 5c). On the other hand, in those sectors, the R1 intensity reveals just the opposite tendency (Figures 1c and 1d), and the occurrence ratio of the R2 intensity is basically the same under the illuminated and unilluminated conditions (Figures 2c and 2d). On the dawn side, in contrast, both R1 and R2 densities consistently show the dayside tendency.

[24] Figure 6 provides a summary of this subsection, which shows the MLT profiles of the R1 (left) and R2 (right) intensities (top) and densities (middle) for the illuminated (solid) and unilluminated (shaded) events. In addition we included in Figure 6 the MLT profiles of the FAC sheet width (bottom). The median values of those quantities in each 2-hour MLT sector are plotted against the corresponding median values of MLT. The number of events in each sector is so large that expected errors for the medians are similar to or less than the size of the markers. We emphasize that Figure 6 is meant to compare the FAC characteristics between the illuminated and unilluminated events at different MLT's but not to address the MLT dependence of the characteristics of the large-scale
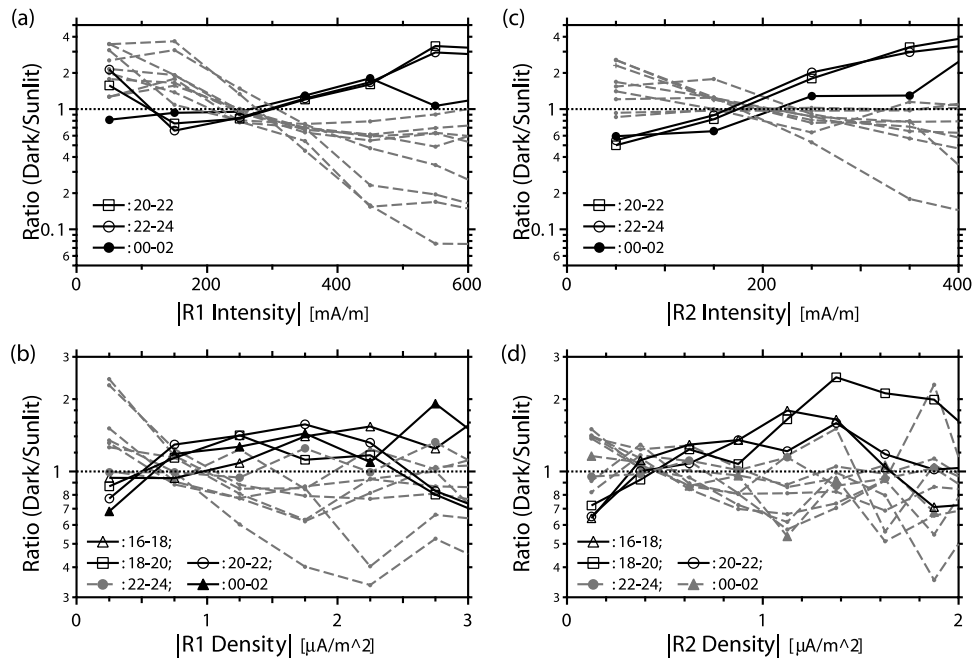
Figure 3. Ratio of the occurrence ratio of the (a) R1 intensity, (b) R1 density, (c) R2 intensity, and (d) R2 density under the dark condition to that under the sunlit condition. Absolute values are used for the intensities and densities of downward FACs. Selected MLT sectors are denoted by different marks in each panel.

FACs; it is possible that the skimming spacecraft orbit in the postnoon and early morning sectors (section 2) causes biases in the FAC intensity and density in those sectors. In fact, the postnoon peak of the R1 and R2 current intensities reported previously [*Iijima and Potemra*, 1976, 1978] cannot be identified in Figure 6.

[25] In each panel we included results for two additional sectors, one on the dayside and the other on the night side, on the opposite side of the noon-midnight meridian for each of the morning-side and evening-side FAC structures. We did this for the night side because the distributions of the R1 and R2 currents can be significantly distorted when geomagnetic activity is high [*Iijima and Potemra*, 1978]. For the midday sector we cannot unambiguously identify the FAC system only from its polarity because the R2 current often disappears there and the demarcation of the prenoon- and postnoon-side R1 and R0 moves across the noon meridian depending on the IMF B_Y component [e.g., *Erlandson et al.*, 1988]. This uncertainty can be avoided if the FAC structure has three sheets; for such events, the FACs can be identified confidently as R2, R1, and R0 currents from equatorward to poleward. For the two midday sectors ($10 \leq$ MLT < 12 and $12 \leq$ MLT < 14) the results exclusively for the three-sheet events are presented by the numbers (0, 1, and 2), which correspond to the FAC identities.

[26] On the dayside the absolute values of the median FAC intensities are significantly larger for the illuminated events than for the unilluminated events (Figures 6a and 6d). This also holds for each FAC system of three-sheet structure events, although its intensity does not necessarily agree with the corresponding value based on the entire events. The tendency is just the opposite for both R1 and R2 intensities at $20 \leq$ MLT < 02. We can find a similar tendency for the

FAC density (Figures 6b and 6e) except that the nightside tendency can be seen at earlier MLT's, even at the evening flank ($16 \leq$ MLT < 18); compare Figure 6a with Figure 6b and Figures 6d with Figure 6e. These features are consistent with what we found for the occurrence ratios of the FAC intensity and density.

[27] The FAC density is calculated by dividing the FAC intensity by the width of the FAC sheet. Therefore the fact that the FAC density reveals different or less clear preferences for the ionospheric conditions suggests that the FAC sheet width is different for the illuminated and unilluminated events. In fact, Figures 6c and 6f show that in most MLT sectors, the FAC sheet is wider for the illuminated events than for the unilluminated events. This explains why the preference for the dark ionosphere is less clear for the FAC density than for the FAC intensity. The tendency appears to be the opposite for the R1 current in the midnight sector and the R2 current in the midnight-dawn sector, which also accounts for the difference between the FAC intensity and density in the MLT sector (the duskward shift of the latter relative to the former) in which the dark ionosphere is preferable for large events. In section 4.1, we will show that those tendencies can be explained, to some extent but not fully, in terms of the magnetospheric configuration.

3.2. Dependence on IMF B_Z

[28] We found that in the evening-to-midnight sector, the FAC tends to be more intense when the ionospheric foot point is dark than when it is sunlit. This result suggests that the ionospheric conductivity plays a different role in that local time sector than in other sectors. However, an additional test is required for verifying this. There are two factors that control the solar zenith angle at the foot point
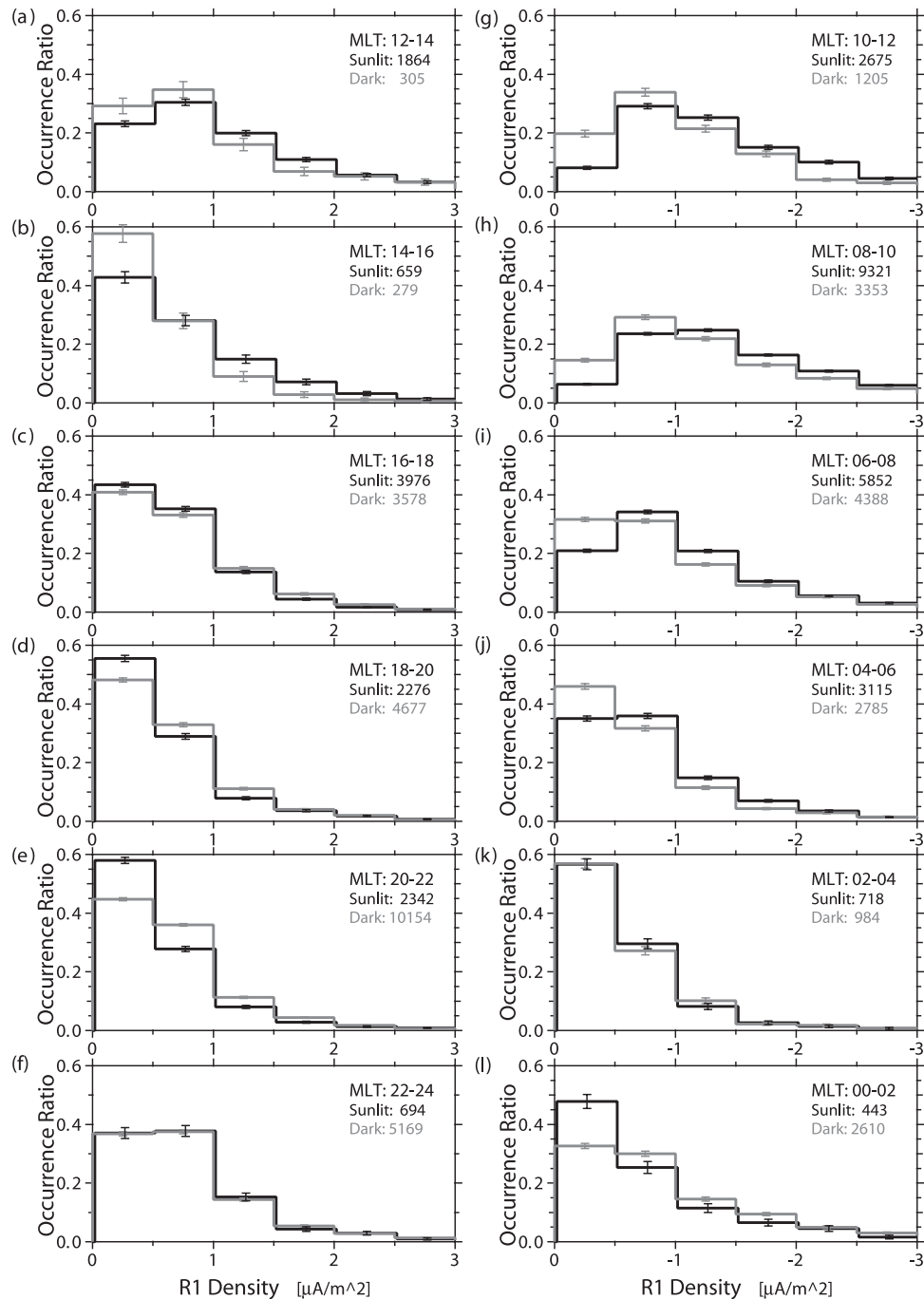
Figure 4. (a–l) Comparison of the R1 current density between the illuminated (solid) and unilluminated (shaded) events in the same format as Figure 1.

of the FAC. The most obvious factor is the dipole tilt. On the night side, the probability that the ionospheric foot point is sunlit increases as the dipole axis is more tilted toward the Sun in the same hemisphere. The other factor is the geomagnetic latitude of the FAC. For a given dipole tilt angle, the probability increases as the geomagnetic latitude of the FAC becomes higher. It is therefore possible that the illuminated events on the night side were selected preferably when FACs were located at higher latitudes. Additional complication arises from the fact that the average latitude of nightside FACs is lower in summer than in winter by as

much as 4° (paper 1), and the FAC has to move even more poleward from the average latitude for its ionospheric foot point to be sunlit. Since FACs tend to move poleward when geomagnetic activity is low [Kamide and Akasofu, 1974; Higuchi and Ohtani, 2000a], our selection of nightside illuminated events may be biased to intervals of low geomagnetic activity, and this could be the reason the FAC intensity and density tend to be smaller for the illuminated events than for the unilluminated events. To verify that the present result is not an artifact of the event selection, we compared the two event sets in terms of the
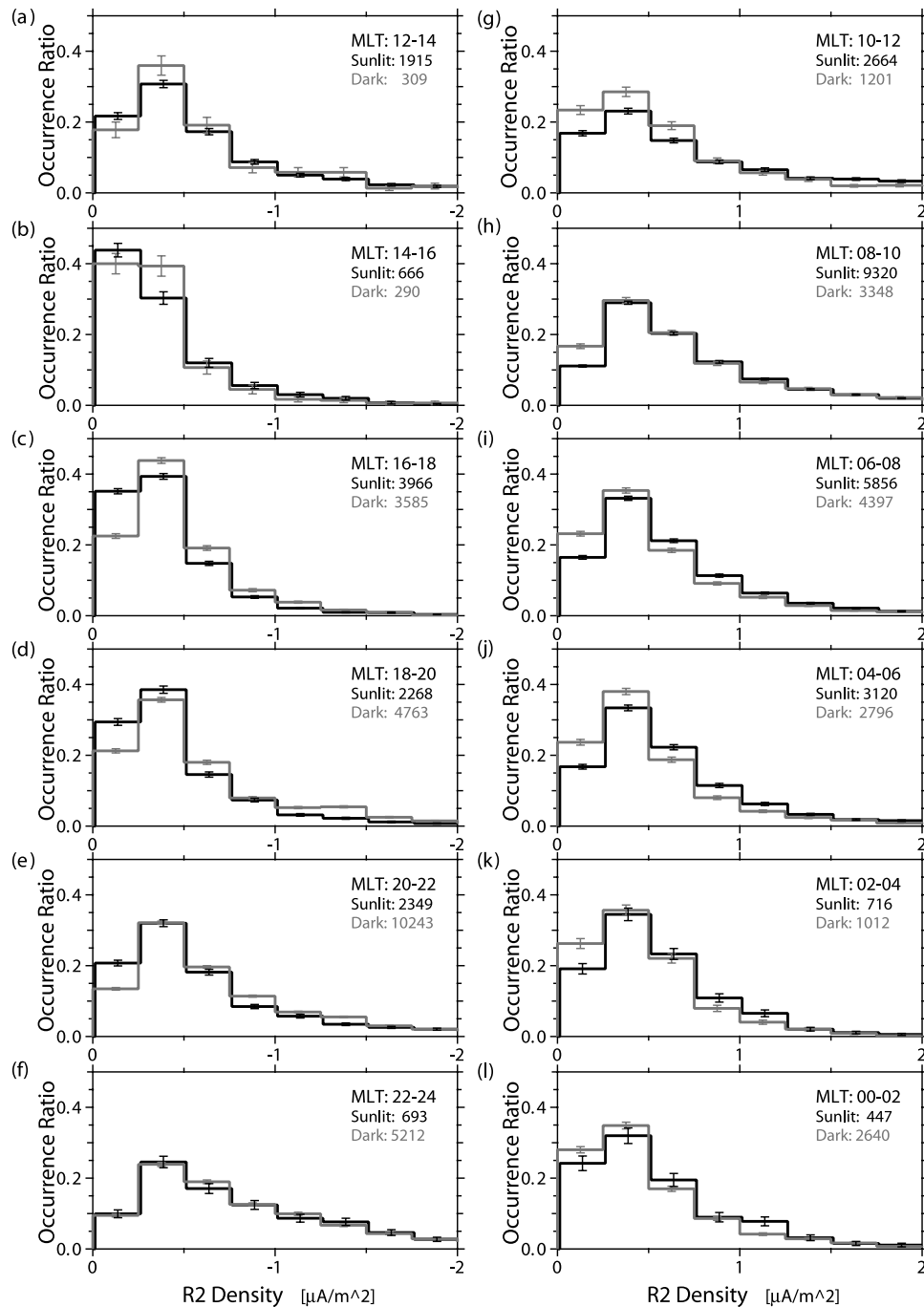
Figure 5. (a–l) Comparison of the R2 current density between the illuminated (solid) and unilluminated (shaded) events in the same format as Figure 1.

IMF B_Z component, which may be used as a measure of geomagnetic activity. We avoided using conventional geomagnetic indices such as AL and AE because those indices also depend on the ionospheric condition [*Ahn et al.*, 2000] and therefore cannot be used as an independent measure.

[29] Figure 7 plots the R1(left) and R2 (right) current intensities (top) and densities (bottom) for the illuminated (solid) and unilluminated (shaded) events against IMF B_Z for $20 \leq$ MLT < 22. This is one of the local time sectors for which we found that the occurrence of intense/strong FACs consistently prefers the dark ionosphere. The values of IMF

B_Z are binned into every 2 nanoteslas, and the median values are used for both the FAC intensity/density and IMF B_Z. Error bars represent ranges between the 16 and 84 percentile points ($\pm 1\sigma$ from the median value) divided by the square root of the number of events. For IMF B_Z, we use 30-min averages of IMP 8 magnetometer data before the events. Propagation time from the satellite position to the subsolar point was taken into account.

[30] For both R1 and R2 currents, the FAC intensity is consistently larger for the unilluminated events than for the illuminated events irrespective of the sign and magnitude of
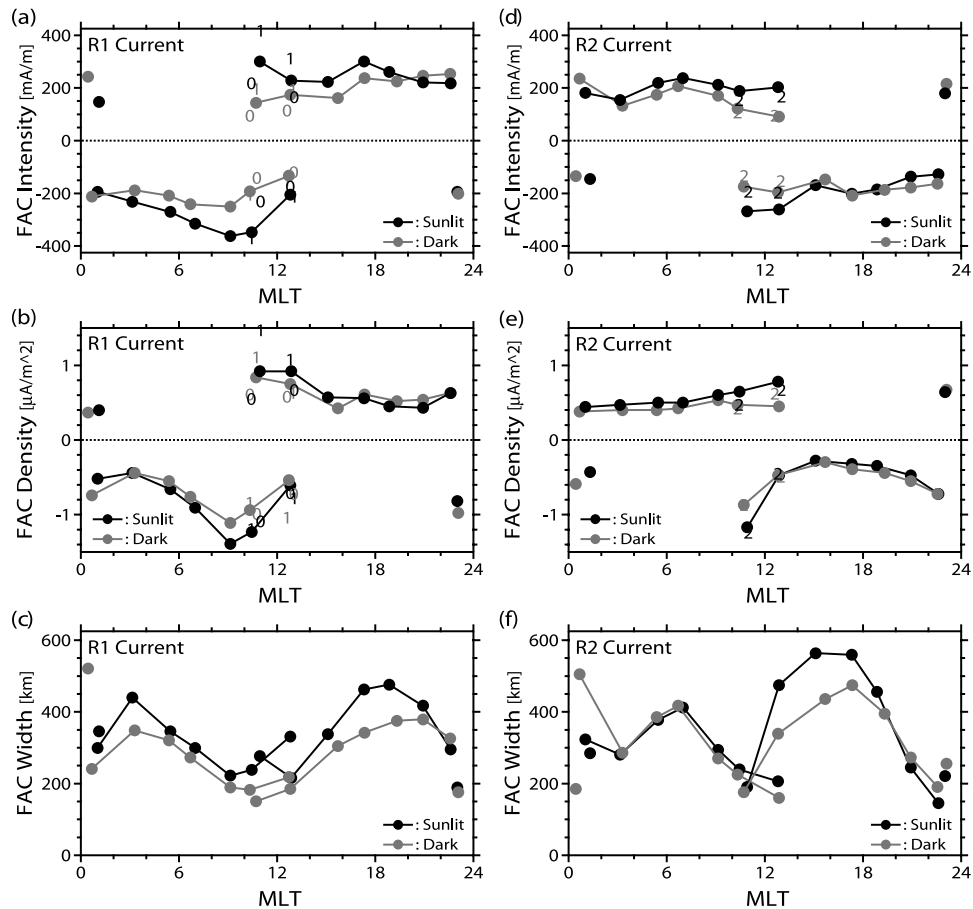
Figure 6. Median (top) intensities, (middle) densities, and (bottom) widths of the (left) R1 and (right) R2 currents for the illuminated (solid) and unilluminated (shaded) events plotted against MLT. See text for details.

IMF B_Z (Figures 7a and 7c). This is also the case for the R1 and R2 densities although there are a few exceptional points (Figures 7b and 7d). The result strongly suggests that the dependence of the nightside FAC intensity/density on the ionospheric condition is a manifestation of a certain M-I coupling process. For the unilluminated events, the FAC intensity/density tends to increase as the IMF becomes more southward, whereas such a tendency is not clear for the
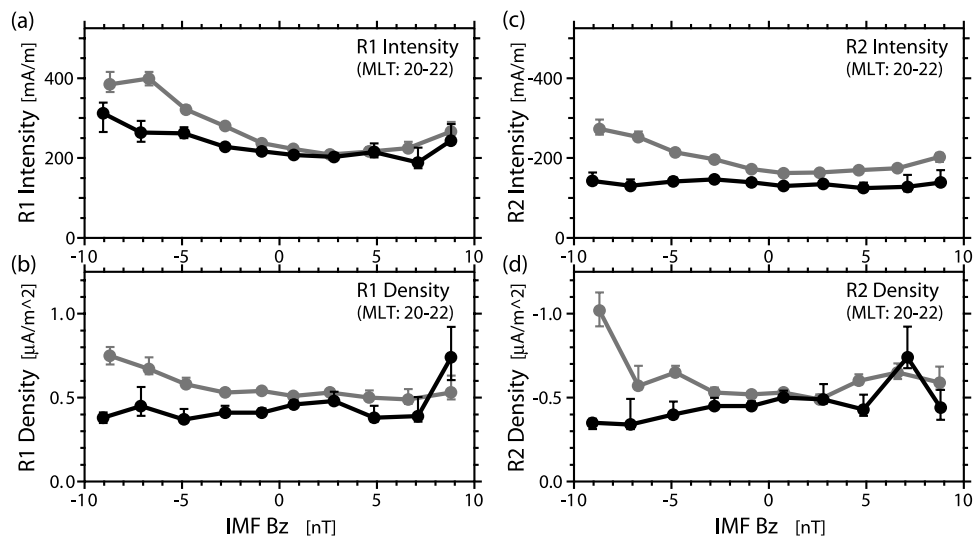

Figure 7. R1 (a) intensity and (b) density and R2 (c) intensity and (d) density versus IMF B_Z for $20 \leq$ MLT < 22. The solid and shaded lines are for the illuminated and unilluminated events, respectively.

illuminated events except for the R1 intensity, which gradually but systematically increases with the southward IMF B_Z. Accordingly the difference between the two event sets is small when IMF B_Z is positive, and it tends to increase as IMF B_Z becomes more negative; this is also the case for the R1 intensity. We therefore infer that the M-I coupling process that prefers the dark ionospheric condition operate more effectively when geomagnetic activity is high and that it is likely related to the substorm.

[31] It is also possible that the IMF B_Z systematically differs between the illuminated and unilluminated events for the dayside FAC. The auroral oval, or the dayside cusp, moves poleward when the IMF B_Z is northward [*Burch*, 1973; *Newell et al.*, 1989], which is preferable for the ionospheric foot point of FACs to be dark. Thus the occurrence of dayside unilluminated events might be biased to positive IMF B_Z and therefore to lower geomagnetic activity. However, we confirmed in the same way that the difference is significant irrespective of the sign or magnitude of IMF B_Z (not shown).

4. Discussion

4.1. Magnetospheric Configuration: FAC Intensity Versus FAC Density

[32] Before we discuss the present result in terms of the M-I coupling, we would like to address the difference between the FAC intensity and density. In section 3.1, we found that the dependence on the ionospheric condition is more significant for the FAC intensity than for the FAC density. This can be attributed at least partly to the fact that the width of the FAC sheet differs for different ionospheric conditions (Figure 6). In most MLT sectors, the FAC sheet is wider for the illuminated events than for the unilluminated events, but the tendency appears to be the opposite, at least not clear, near midnight (Figures 6c and 6f). In this subsection we will discuss the width of the FAC sheet in terms of the magnetospheric configuration.

[33] The tilt of the dipole axis not only determines the condition (illuminated or unilluminated) at the ionospheric foot point but also affects the characteristics of large-scale FAC systems through the magnetospheric configuration. Using the Tsyganenko 96 (T96) model [*Tsyganenko*, 1996] with the tilted dipole axis corresponding to the summer solstice (Figure 8a), we traced field lines toward the northern and southern ionospheres from the magnetic equatorial plane at ($r =$) 6, 8, and 10 R_E from the Earth; here we assumed P_{dyn} (solar wind dynamic pressure) = 3 nPa, Dst = 0 nT, IMF B_Y = 0 nT, and IMF B_Z = 0 nT. Figure 8b plots the absolute latitudes of northern (solid) and southern (dashed) foot points against MLT. The segments superposed to the $r = 10$ R_E foot points connect conjugate points for every one hour in MLT at the geomagnetic equator.

[34] The latitudinal separation between the foot points of the $r = 8$ and $r = 10$ R_E field lines is smaller in the summer (northern) hemisphere than in the winter (southern) hemisphere on the night side. That is, as we trace a flux tube from the nightside equator toward the Earth, it is more pinched in the latitudinal direction in the summer hemisphere than in the winter hemisphere. Since the total magnetic flux must be conserved, this means that the flux tube becomes more elongated in the longitudinal direction
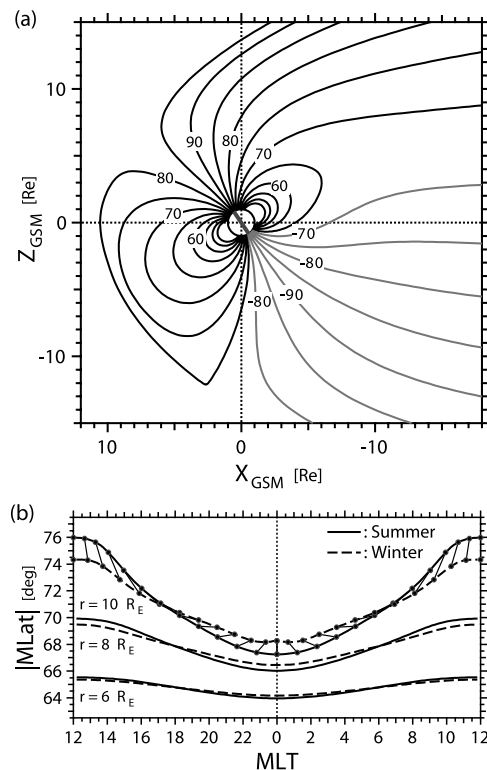

Figure 8. (a) *X-Z* cross section of the Tsyganenko 96 model (P_{dyn} = 3 nPa, Dst = 0 nT, IMF B_Y = 0 nT, and IMF B_Z = 0 nT) with the dipole approximation for the internal field for the summer solstice. Solid and shaded lines are traced from the northern and southern ionospheres, respectively. This figure is adopted from Figure 11b of paper 1. (b) Northern and southern foot points of field lines traced from different geomagnetic equatorial distances ($r = 6$, 8, and 10 R_E) using the model magnetic field of Figure 8a. The conjugate points of the $r = 10$ R_E field lines are connected by the segments for every 1 hour in MLT at geomagnetic equator. This figure is based on the same calculation as presented in Figure 12 of paper 1 except the horizontal axis is centered at midnight instead of noon.

in the summer hemisphere. Accordingly, as shown by the segments on the night side, field lines are mapped farther away from midnight in the summer ionosphere than in the winter ionosphere. For example, the equatorial point at $r = 10$ R_E and MLT = 1.0 is traced to the summer ionosphere at MLT = 1.18 and to the winter hemisphere at MLT = 0.65. The interhemispheric difference decreases with decreasing dipole tilt angle, and it increases with increasing southward IMF B_Z (not shown). We also emphasize that the radial distance range, $r \sim 10$ R_E, considered here typically corresponds to the source region of the R2 system [*Iijima et al.*, 1990], and the interhemispheric difference could be even larger for the R1 system, the source of which is located farther down the tail.

[35] Assume that the same amount of electric current flows toward the summer and winter ionospheres from the plasma sheet (or the ring current) along a certain flux tube and that there is no additional source or sink of FAC. The FAC density is inversely proportional to the cross section of the flux tube and so is the total magnetic field strength. Thus

the FAC density should be the same at the two ionospheric foot points as far as the total magnetic field strength is the same. On the other hand, since the corresponding ionospheric cross section is azimuthally more elongated in the summer hemisphere than in the winter hemisphere, the local FAC intensity, which is defined as the total current across the current sheet, is smaller in the summer hemisphere than in the winter hemisphere. The tendency is consistent with our result that the nightside FAC intensity tends to be smaller for the illuminated events than for the unilluminated events; the occurrence of the former should be confined in the local summer.

[36] On the dayside everything works qualitatively in the opposite way and quantitatively less significantly. The traces of the foot points for different radial distances are less separated in latitude in the winter hemisphere than in the summer hemisphere. Accordingly, the flux tube is more pinched latitudinally and is more elongated azimuthally as is traced to the winter ionosphere than toward the summer ionosphere. From $r = 10$ R_E and MLT = 11, the field line is traced to MLT = 11.14 and 11.35 in the winter and summer ionospheres, respectively. Thus, if the total FAC is the same, the local FAC intensity above the ionosphere should be larger in the summer hemisphere.

[37] The fact that the interhemispheric asymmetry is less obvious for the FAC density than for the FAC intensity suggests that this geometrical effect is important especially for the night side. Nevertheless, the FAC density reveals a similar preference for the ionospheric condition as the FAC intensity. Furthermore, the MLT sector where the occurrence of large FAC densities prefers the dark ionosphere is significantly skewed toward evening. These results cannot be explained in terms of the magnetospheric configuration, and therefore we infer that they reflect a certain M-I coupling process.

4.2. Dependence of FAC Intensity/Density on the Ionospheric Conductivity

[38] Regarding the dayside FAC, we found that intense FACs tend to take place when the ionosphere is sunlit. This is consistent with the results of the previous studies and has been widely explained in terms of the solar EUV contribution to the ionospheric conductivity [*Fujii et al.*, 1981; *Fujii and Iijima*, 1987; *Ohtani et al.*, 2000, 2005; *Christiansen et al.*, 2002; *Haraguchi et al.*, 2004]. The solar illumination is the primary cause of ionospheric ionization in the afternoon sector. In the prenoon sector, it is one of the two major causes of the ionization along with diffuse (unaccelerated) electron precipitation [*Newell et al.*, 1996, Figure 2]. Therefore it should be reasonable that more current flows through the sunlit ionosphere than through the dark ionosphere as far as FACs in two hemispheres share the same source (if FACs flow on closed field lines) or have sources with similar strengths (if FACs flow on open field lines).

[39] In contrast to the dayside FAC, the dependence of the nightside FAC on the ionospheric condition (or season) is unclear in the results of the past studies. *Fujii et al.* [1981] did not find any significant difference in the nightside FAC intensity between summer and winter events. *Fujii and Iijima* [1987] reported that the nightside FAC intensity is positively, rather than negatively, correlated with the solar-

induced ionospheric conductivity. Those results appear to disagree with our finding that in the evening-to-midnight sector, the FAC is more intense under the dark condition than under the sunlit condition. However, this apparent discrepancy can be explained in terms of the local time coverage of the data sets. *Fujii et al.* [1981] and *Fujii and Iijima* [1987] used magnetometer data from the TRIAD and MAGSAT satellites, respectively, and neither data set covers the premidnight sector. For example, the latest evening sector covered by the MAGSAT data set was 18–20 in MLT.

[40] *Christiansen et al.* [2002] compared characteristics of nightside large-scale FACs observed by the Ørsted satellite in northern winter and southern summer. Nightside events they examined are distributed mostly in the premidnight sector. Nevertheless, their study suggested no systematic interhemispheric difference in the FAC intensity or density. This might be attributed to a limited time interval of their event set, which covers only a single season.

[41] In paper 1 we found that the nightside R2 intensity tends to increase as the dipole axis tilts away from the Sun in the same hemisphere (Figure 8 of paper 1). However, we could not find any corresponding tendency for the R1 intensity. This might be explained in terms of the occurrence frequency of illuminated events on the night side. For the nightside ionosphere to be sunlit, the dipole axis has to be most tilted toward the Sun, and accordingly such events constitute only a small fraction of the entire events; see the number of events inserted in each panel of Figures 1, 2, 4, and 5. Thus, if all events are used for a linear regression analysis as was done in paper 1, the FAC suppression in the illuminated events may be masked by the overwhelming majority of the unilluminated events. However, it still remains to be understood why the R2 intensity systematically depends on the dipole tilt angle.

[42] Interestingly, the polar distributions of the FAC density reported by *Weimer* [2001] and *Papitashvili et al.* [2002] provide hints for different conductivity dependences of large-scale FAC systems between the dusk-to-midnight and postmidnight-to-dawn sectors. Those studies examined polar distributions of the FAC density for different IMF clock angles for northern winter and southern summer; see *Weimer* [2001, Figures 3 and 4] and *Papitashvili et al.* [2002, Figure 3]. Careful visual inspection of their results reveals that the contours of the evening-side R2 and R1 density shift along with their peaks toward later local times in winter, although the difference of the local FAC density itself is not clear. In the postmidnight-morning sector, in contrast, the FAC density is noticeably higher in summer than in winter, which is also consistent with the present result. Those seasonal dependences can also be recognized in the result of T. Hasunuma et al. (Polar distributions of small-scale field-aligned currents and their relationship to the large-scale field-aligned current system, submitted to *Journal of Geophysical Research*, 2005), although the overall distribution of the FAC density is significantly skewed toward nightside.

4.3. M-I Coupling: Feedback Instability

[43] The FAC and auroral acceleration are closely related to each other (the Knight relation [*Knight*, 1973]). For the dusk-to-premidnight sector, the preferred occurrence of

intense events under the dark condition has been reported for electron acceleration [*Newell et al.*, 1996], auroral brightness [*Liou et al.*, 1997; *Shue et al.*, 2001], energy of auroral electrons [*Liou et al.*, 2001], and electrostatic shocks [*Bennett et al.*, 1983]. For the postmidnight sector, in contrast, such preference can be found for intense ion precipitation [*Newell et al.*, 2005] and diverging electric field [*Marklund et al.*, 1997]. The former set of features is associated with the upward FAC, and the latter set with the downward FAC. In section 3.1 we found that the upward R1 current at $16 \leq$ MLT < 22 and the downward R1 current at $00 \leq$ MLT < 02 tend to be stronger when the ionosphere is dark than when it is sunlit. This result appears to provide a missing piece of the physical link between the magnetosphere and the ionosphere, which, however, needs to be carefully addressed.

[44] The preferred occurrence of intense M-I coupling for the low ionospheric conductivity is often explained in terms of the feedback instability, which has been considered to explain the formation of discrete auroral arcs [*Atkinson*, 1970; *Sato*, 1978; *Miura and Sato*, 1980; *Lysak*, 1991; *Lysak and Song*, 2002]. This instability results from the change in the ionospheric conductivity caused by downward field-aligned transport of electrons (and additional ionization by such electrons). In the presence of a background electric field, the resultant spatial gradient of the ionospheric conductivity causes a secondary FAC. This secondary FAC is carried by an Alfvén wave, which propagates upward from the ionosphere, and then is reflected at the conjugate ionosphere [*Atkinson*, 1970; *Sato*, 1978; *Miura and Sato*, 1980] or at the sharp gradient of the Alfvén velocity above the ionosphere [*Lysak*, 1991]. If the phase of the reflected wave is such that it enhances the original change of the conductivity, the perturbation grows. The required phase matching between the reflected wave and the advection of the original conductivity variation at the ionosphere determines the perpendicular wavelength at the ionosphere, which was found to be consistent with the formation of discrete arcs. As the background conductivity becomes lower, the Alfvén wave contributes more to the closure of the ionospheric current, which is preferable for the instability. It should be noted that the feedback instability can also operate for the downward FAC [*Streltsov and Lotko*, 2003]. The downward FAC removes electrons from the ionosphere reducing the local conductivity and therefore it sets up a favorable condition for the instability.

[45] It is tempting to interpret the result of the present study in terms of the feedback instability. However, there are at least two issues that require careful consideration. First, it is questionable whether the feedback instability can operate in such a large scale as the entire scale of large-scale FACs, which is at least $1°$ (or 100 km) in latitude. This instability has been considered to explain the formation of auroral arcs, the latitudinal scale of which is generally much smaller than that of large-scale FAC sheets. The typical latitudinal scale of inverted V precipitation is a fraction of degree [e.g., *Lin and Hoffman*, 1979], and that of intense electric fields is less than 10 km [*Mozer et al.*, 1980; *Marklund et al.*, 1997]. Modeling studies of the feedback instability show the growth of perturbations with latitudinal scales comparable to the observation [*Sato*, 1978; *Miura and Sato*, 1980; *Lysak and Song*, 2002; *Streltsov and Lotko*,

2003]. Therefore, although the associated FACs may result in more structured latitudinal profiles of the FAC density, it is not clear whether it changes the mean density or the total intensity of large-scale FACs.

[46] Another issue of applying the feedback instability to the present result is that the dark ionosphere is favorable for the occurrence of not only strong (large-density) R1 currents but also strong R2 currents. As for the R2 current, however, such preference can be found only for the downward current in the evening-to-premidnight sector (Figure 5) but not for the upward current in the postmidnight sector. In contrast, diverging electric fields and intense ion precipitation, which are possible manifestations of the feedback instability for the downward FAC, are observed more frequently in the postmidnight sector than in the evening sector [*Marklund et al.*, 1997; *Newell et al.*, 2005], presumably in association with the downward R1 current; we also found that the downward R1 current density at $00 \leq$ MLT < 02 tends to be larger when the ionosphere is dark than when it is sunlit (Figure 4). Furthermore, in general, particle precipitation is less structured in the R2 current than in the R1 current [*Sanchez et al.*, 1993]. It is therefore not clear whether the preferred occurrence of strong R2 currents in the evening-to-premidnight sector under the dark condition can be explained in terms of the feedback instability.

[47] From the viewpoint of energy budget, it is reasonable that the R2 current intensifies in the same local time sector as the R1 current so that the enhanced current can be closed latitudinally in the ionosphere. In such a way the total Joule dissipation in the ionosphere can be reduced. On the other hand, if only the R1 current intensifies but the R2 current does not, the excess upward R1 current has to be closed with a downward current at a different local time, for which the ionospheric closure current must flow a long distance resulting in more Joule dissipation. Therefore the dependence of the large-scale FAC systems on the ionospheric condition may need to be addressed from a global as well as a local point of view.

4.4. Semiannual Variations of Geomagnetic Activity

[48] Finally, we would like to comment on the semiannual variation of geomagnetic activity in terms of the global FAC intensity. It is well known that geomagnetic activity is statistically higher at the equinoxes than at the solstices [e.g., *Russell and McPherron*, 1973; *Berthelier*, 1976; *Cliver et al.*, 2000; *O'Brien and McPherron*, 2002], although its cause is rather controversial [*Cliver et al.*, 2000].

[49] The present result suggests that the total amount of FACs closing in the evening-to-midnight sectors of the northern and southern ionospheres is larger if both hemispheres are dark; this is especially the case when the external condition is favorable for high geomagnetic activity (section 3.2). Such an ionospheric condition is met most easily around the equinoxes.

[50] On the dayside, in contrast, the solar illumination is favorable for the occurrence of intense FACs. Around the equinoxes the dayside auroral zone is most likely sunlit in both hemispheres, whereas around the solstices it is often dark in one hemisphere. Thus, again, the total FAC on the dayside is inferred to be larger around the equinoxes. This idea needs to be examined quantitatively since the solar-induced ionospheric conductivity is a function of the solar

zenith angle and presumably so is the FAC intensity. However, as far as the conductivity decreases more sharply with the solar zenith angle as it approaches 90° [*Robinson and Vondrak*, 1984; *Moen and Brekke*, 1993], the sum of the northern and southern ionospheric conductivities on the dayside, which may be regarded as an effective conductivity for the global M-I coupling, is larger around the equinoxes than around the solstices; see *Ebihara et al.* [2004, Figure 7]. This favors the idea.

[51] Thus the global FAC intensity, the FAC integrated over auroral zones in both hemispheres, is expected to vary semiannually with its maxima at the equinoxes and its minima at the solstices. It is most plausible that geomagnetic activity is correlated with the global FAC intensity, and therefore the dependence of the FAC intensity on the ionospheric condition possibly makes an additional contribution to the semiannual variation of geomagnetic activity.

5. Summary

[52] In the present study we statistically examined how large-scale field-aligned currents (FACs) depend on the solar-induced ionospheric conductivity. We selected a total of ~74,000 crossings from magnetic field measurements made by the DMSP F7 and F12 to F15 satellites, requiring that the ionospheric footprint of the entire orbital segment during the crossing of large-scale FACs is either sunlit or dark. The illuminated and unilluminated events are compared in terms of the occurrence of the FAC intensity and density for each 2-hour bin of MLT. We found that the intensities and densities of dayside R1 and R2 currents are statistically larger for the illuminated events than for the unilluminated events, which is consistent with the results of the previous studies. For the nightside FAC, in contrast, we addressed for the first time a few important features with statistical confidence thanks to our large event set. We found that (1) At $20 \leq$ MLT < 02 the intensities of both R1 and R2 currents tend to be larger under the dark condition than under the sunlit condition; (2) The dependence on the ionospheric condition is less clear for the FAC density, but the preferred occurrence of strong FACs for the dark ionosphere can be found for both R1 and R2 currents in the dusk-to-premidnight ($16 \leq$ MLT < 22) sector and the R1 current in the postmidnight sector ($00 \leq$ MLT < 02); and (3) For both FAC intensity and density, the difference between the illuminated and unilluminated events tends to increase with increasing geomagnetic activity as measured by the IMF B_Z component. We suggested that the interhemispheric asymmetry of the magnetospheric configuration is important for the (apparent) dependence of the FAC intensity on the ionospheric condition. The ionospheric cross section of a magnetic flux tube is latitudinally wider in the winter (dark) hemisphere than in the summer (sunlit) hemisphere and therefore, even for the same FAC density, the FAC intensity can be larger in the winter hemisphere as the FAC intensity is an integral of the FAC density across the FAC sheet. This explains why the dependence on the ionospheric condition (illuminated or unilluminated) is more obvious for the FAC intensity than for the FAC density. However, the fact that the occurrence of the larger FAC density also prefers the dark ionosphere strongly suggests that the solar-induced

conductivity controls the M-I coupling in a different way in certain local time sectors on the night side. Similar preferences for the dark ionosphere have been reported for intense particle precipitation, bright aurorae, and intense electric fields, which are often explained in terms of the feedback instability. However, it is not clear whether this instability applies to the present result since the latitudinal scale of large-scale FACs is significantly larger than the scale of those other features. We also pointed out that the low (solar-induced) ionospheric conductivity is preferable for the occurrence of not only strong R1 currents but also strong R2 currents, which we may need to address from the perspective of global energy budget, that is, Joule dissipation owing to the ionospheric closure current. We also suggested that the dependence of the FAC intensity on the ionospheric condition might contribute to the semiannual variation of geomagnetic activity.

References

Ahn, B.-H., H. W. Kroehl, Y. Kamide, and E. A. Kihn (2000), Seasonal and solar cycle variations of the auroral electrojet indices, *J. Atmos. Sol. Terr. Phys.*, *62*, 1301.

Atkinson, G. (1970), Auroral arcs: Result of the interaction of a dynamic magnetosphere with the ionosphere, *J. Geophys. Res.*, *75*, 4746.

Baker, K. B., and S. Wing (1989), A new magnetic coordinate system for conjugate studies at high latitude, *J. Geophys. Res.*, *94*, 9139.

Bennett, E. L., M. Temerin, and F. S. Mozer (1983), The distribution of auroral electrostatic shocks below 8000-km altitude, *J. Geophys. Res.*, *88*, 7107.

Berthelier, A. (1976), Influence of the polarity of the interplanetary magnetic field on the annual and the diurnal variations of magnetic activity, *J. Geophys. Res.*, *81*, 4546.

Borovsky, J. E., and H. O. Funsten (2003), Role of solar wind turbulence in the coupling of the solar wind to the Earth's magnetosphere, *J. Geophys. Res.*, *108*(A6), 1246, doi:10.1029/2002JA009601.

Burch, J. L. (1973), Rate of erosion of dayside magnetic flux based on a quantitative study of the dependence of polar cusp latitude on the interplanetary magnetic field, *Radio Sci.*, *8*, 955.

Cattell, C. A., J. Dombeck, W. Yusof, C. Carlson, and J. McFadden (2004), FAST observations of the solar illumination dependence of upflowing electron beams in the auroral zone, *J. Geophys. Res.*, *109*, A02209, doi:10.1029/2003JA010075.

Christiansen, F., V. O. Papitashvili, and T. Neubert (2002), Seasonal variations of high-latitude field-aligned currents inferred from Orsted and MAGSAT observations, *J. Geophys. Res.*, *107*(A2), 1029, doi:10.1029/2001JA900104.

Cliver, E. W., Y. Kamide, and A. G. Ling (2000), Mountains versus valleys: Semiannual variation of geomagnetic activity, *J. Geophys. Res.*, *105*, 2413.

Ebihara, Y., M.-C. Fok, R. A. Wolf, T. J. Immel, and T. E. Moore (2004), Influence of ionosphere conductivity on the ring current, *J. Geophys. Res.*, *109*, A08205, doi:10.1029/2003JA010351.

Elphic, R. C., J. Bonnell, R. J. Strangeway, C. W. Carlson, M. Temerin, J. P. McFadden, R. E. Ergun, and W. Peria (2000), FAST observations of upward accelerated electron beams and the downward field-aligned current region, in *Magnetospheric Current Systems, Geophys. Monogr. Ser.*, vol. 118, edited by S. Ohtani et al., p. 173, AGU, Washington, D. C.

Erlandson, R. E., L. J. Zanetti, T. A. Potemra, P. F. Bythrow, and R. Lundin (1988), IMF B_Y dependence of region 1 Birkeland currents near noon, *J. Geophys. Res.*, *93*, 9804.

Fujii, R., and T. Iijima (1987), Control of the ionospheric conductivities on large-scale Birkeland current intensities under geomagnetic quiet conditions, *J. Geophys. Res.*, *92*, 4505.

Fujii, R., T. A. Potemra, and M. Sugiura (1981), Seasonal dependence of large-scale Birkeland current intensities under geomagnetic quiet conditions, *Geophys. Res. Lett.*, *8*, 1103.

Haraguchi, K., H. Kawano, K. Yumoto, S. Ohtani, T. Higuchi, and G. Ueno (2004), Ionospheric conductivity dependence of dayside region-0, 1, and 2 field-aligned current systems: Statistical study with DMSP-F7, *Ann. Geophys.*, *22*, 2775.

Higuchi, T., and S. Ohtani (2000a), Automatic identification of large-scale field-aligned current structures and its application to night-side FAC systems, in *Magnetospheric Current Systems*, *Geophys. Monogr. Ser.*, vol. 118, edited by S. Ohtani et al., p. 389, AGU, Washington, D. C.

Higuchi, T., and S. Ohtani (2000b), Automatic identification of large-scale field-aligned current structures, *J. Geophys. Res.*, *105*, 25,305.

Iijima, T., and T. A. Potemra (1976), The amplitude distribution of field-aligned currents at northern high latitudes observed by TRIAD, *J. Geophys. Res.*, *81*, 2165.

Iijima, T., and T. A. Potemra (1978), Large-scale characteristics of field-aligned currents associated with substorms, *J. Geophys. Res.*, *83*, 599.

Iijima, T., T. A. Potemra, and L. J. Zanetti (1990), Large-scale characteristics of magnetospheric equatorial currents, *J. Geophys. Res.*, *95*, 991.

Kamide, Y., and S.-I. Akasofu (1974), Latitudinal cross section of the auroral electrojet and its relation to the interplanetary magnetic field polarity, *J. Geophys. Res.*, *79*, 3755.

Knight, S. (1973), Parallel electric fields, *Planet. Space Sci.*, *21*, 741.

Lin, C. S., and R. A. Hoffman (1979), Characteristics of the inverted-V event, *J. Geophys. Res.*, *84*, 1514.

Liou, K., P. T. Newell, C.-I. Meng, M. Brittnacher, and G. Parks (1997), Synoptic auroral distribution: A survey using Polar ultraviolet imagery, *J. Geophys. Res.*, *102*, 27,197.

Liou, K., P. T. Newell, and C.-I. Meng (2001), Seasonal effects on auroral particle acceleration and precipitation, *J. Geophys. Res.*, *106*, 5531.

Lyons, L. R. (1980), Generation of large-scale regions of auroral currents, electric potentials, and precipitation by the divergence of the convection electric field, *J. Geophys. Res.*, *85*, 17.

Lyons, L. R. (1981), Discrete aurora as the direct result of an inferred high-altitude generating potential distribution, *J. Geophys. Res.*, *86*, 1.

Lysak, R. L. (1991), Feedback instability of the ionospheric resonant cavity, *J. Geophys. Res.*, *96*, 1553.

Lysak, R. L., and Y. Song (2002), Energetics of the ionospheric feedback interaction, *J. Geophys. Res.*, *107*(A8), 1160, doi:10.1029/2001JA000308.

Marklund, G., T. Karlsson, and J. Clemmons (1997), On low-altitude particle acceleration and intense electric fields and their relationship to black aurora, *J. Geophys. Res.*, *102*, 17,509.

Miura, A., and T. Sato (1980), Numerical simulation of the global formation of auroral arcs, *J. Geophys. Res.*, *85*, 73.

Moen, J., and A. Brekke (1993), The solar flux influence on quiet time conductances in the auroral ionosphere, *Geophys. Res. Lett.*, *20*, 971.

Mozer, F. S., C. A. Cattell, M. K. Hudson, R. L. Lysak, M. Temerin, and R. B. Torbert (1980), Satellite measurements and theories of low-altitude auroral particle acceleration, *Space Sci. Rev.*, *27*, 155.

Newell, P. T., C.-I. Meng, D. G. Sibeck, and R. P. Lepping (1989), Some low-altitude cusp dependencies on the interplanetary magnetic field, *J. Geophys. Res.*, *94*, 8921.

Newell, P. T., C.-I. Meng, and K. M. Lyons (1996), Suppression of discrete aurorae by sunlight, *Nature*, *381*, 766.

Newell, P. T., S. Wing, T. Sotirelis, and C.-I. Meng (2005), Ion aurora and its seasonal variations, *J. Geophys. Res.*, *110*, A01215, doi:10.1029/2004JA010743.

O'Brien, T. P., and R. L. McPherron (2002), Seasonal and diurnal variation of *Dst* dynamics, *J. Geophys. Res.*, *107*(A11), 1341, doi:10.1029/2002JA009435.

Ohtani, S., T. Higuchi, T. Sotirelis, and P. T. Newell (2000), Disappearance of large-scale field-aligned current systems: Implications for the solar wind-magnetosphere coupling, in *Magnetospheric Current Systems*, *Geophys. Monogr. Ser.*, vol. 118, edited by S. Ohtani et al., p. 253, AGU, Washington, D. C.

Ohtani, S., G. Ueno, T. Higuchi, and H. Kawano (2005), Annual and semiannual variations of the location and intensity of large-scale field-aligned currents, *J. Geophys. Res.*, *110*, A01216, doi:10.1029/2004JA010634.

Olsson, A., L. Andersson, A. I. Eriksson, J. Clemmons, R. E. Erlandson, G. Reeves, T. Huges, and J. S. Murphree (1998), Freja studies of the current-voltage relation in substorm-related events, *J. Geophys. Res.*, *103*, 4285.

Papitashvili, V. O., F. Christiansen, and T. Neubert (2002), A new model of field-aligned currents derived from high-precision satellite magnetic field data, *Geophys. Res. Lett.*, *29*(14), 1683, doi:10.1029/2001GL014207.

Rich, F. J., D. A. Hardy, and M. S. Gussenhoven (1985), Enhanced ionosphere-magnetosphere data from the DMSP satellites, *Eos Trans. AGU*, *66*, 513.

Robinson, R. M., and R. R. Vondrak (1984), Measurements of E region ionization and conductivity produced by solar illumination at high latitudes, *J. Geophys. Res.*, *89*, 3951.

Russell, C. T., and R. L. McPherron (1973), Semiannual variation of geomagnetic activity, *J. Geophys. Res.*, *78*, 92.

Sanchez, E. R., B. H. Mauk, P. T. Newell, and C.-I. Meng (1993), Low-altitude observations of the evolution of substorm injection boundaries, *J. Geophys. Res.*, *98*, 5815.

Sato, T. (1978), A theory of quiet auroral arcs, *J. Geophys. Res.*, *83*, 1042.

Shue, J.-H., P. T. Newell, K. Liou, and C.-I. Meng (2001), The quantitative relationship between auroral brightness and EUV Pedersen conductance, *J. Geophys. Res.*, *106*, 5883.

Streltsov, A. V., and W. Lotko (2003), Small-scale electric fields in downward auroral current channels, *J. Geophys. Res.*, *108*(A7), 1289, doi:10.1029/2002JA009806.

Tsyganenko, N. A. (1996), Effects of the solar wind conditions on the global magnetospheric configuration as deduced from data-based field models, *Eur. Space Agency Spec. Publ., ESA SP-389*, 181.

Weimer, D. R. (2001), Maps of ionospheric field-aligned currents as a function of the interplanetary magnetic field derived from Dynamics Explorer 2 data, *J. Geophys. Res.*, *106*, 12,889.

————————————

T. Higuchi and G. Ueno, Institute of Statistical Mathematics, Tokyo 106-8569, Japan.

S. Ohtani, Johns Hopkins University Applied Physics Laboratory, Laurel, MD 20723, USA. (ohtani@jhuapl.edu)